REPORT DOCUMENTATION PAGE

1. REPORT DATE	2. REPORT TYPE	3. DATES COVERED (From - To)
29-Sep-2006	REPRINT	

4. TITLE AND SUBTITLE

MAGNITUDE-YIELD AND TRAVEL-TIME CALIBRATION OF NORTHERN EURASIA USING DEEP SEISMIC SOUNDING DATA SETS

5a. CONTRACT NUMBER
DTRA01-01-C-0057

5b. GRANT NUMBER

5c. PROGRAM ELEMENT NUMBER

6. AUTHOR(S)
Igor B. Morozov[1], Elena A. Morozova[2], Chaoying Zhang[1], Glenn Chubak[1], W. Scott Phillips[3], and Igor A. Lipovetsky[4]

5d. PROJECT NUMBER
DTRA

5e. TASK NUMBER
OT

5f. WORK UNIT NUMBER
A1

7. PERFORMING ORGANIZATION NAME(S) AND ADDRESS(ES)

University of Wyoming
Department of Geology and Geophysics
P.O. Box 3006
Laramie, WY 82071-3006

8. PERFORMING ORGANIZATION REPORT NUMBER

9. SPONSORING / MONITORING AGENCY NAME(S) AND ADDRESS(ES)
Air Force Research Laboratory
29 Randolph Road
Hanscom AFB, MA 01731-3010

10. SPONSOR/MONITOR'S ACRONYM(S)
AFRL/VSBYE

11. SPONSOR/MONITOR'S REPORT NUMBER(S)
AFRL-VS-HA-TR-2006-1101

University of Saskatchewan[1], University of Wyoming[2], Los Alamos National Laboratory[3] and Center GEON/Vniigeophysika[4]

14. ABSTRACT

Travel-time and magnitude-yield calibration of Northern Eurasia, which is largely aseismic, can be improved by using the large chemical and peaceful nuclear explosion (PNEs) seismic data sets that resulted from the Soviet Deep Seismic Sounding (DSS) program. Eleven major data sets of this program have recently been digitized and become available to nuclear test monitoring research. In this study, we extend this database by including the source ground truth parameters (charge types, sizes, and other relevant information where available) of the chemical explosions and digitizing several earthquake data sets acquired along the DSS profiles. For seamless data exchange with the test monitoring community, we incorporate the waveforms and ancillary data into the National Nuclear Security Agency (NNSA) database schema.

To date, we have assembled a database of frequency-dependent coda parameters from the PNEs and performed their preliminary interpretation. By utilizing a newly developed, parallelized version of the one-dimensional (1D) *reflectivity* program, we also extended synthetic modeling to the full DSS frequency band (0.5-20 Hz) in velocity models of realistic crustal complexity. This modeling suggests that compared to the mantle, the crust plays the most significant role in relating the observed coda decay parameter (Q) to the intrinsic (elastic and inelastic) dependence, and also that leaking of the seismic energy into the mantle could account for the strong frequency dependence of the observed coda Q. Based on the resulting empirical relationships, we improve our previous measurements of the bulk crustal $Q(f)$ along profile QUARTZ.

In the ongoing work, we will further utilize the DSS data sets for 1) coda magnitude analysis for chemical and nuclear explosions; 2) derivation of empirical magnitude (apparent coda source spectra) yield relationships for small explosion events; and 3) examination of the variability of the derived coda calibration parameters (particularly crustal attenuation), along and across the profiles, correlating this variability with geology and tectonics of the area. Additionally, the goals of this project include derivation of a P-wave travel-time calibration model for Northern Eurasia with an unusually well-constrained and detailed crustal and uppermost mantle structure based on the chemical explosion data. These efforts should ultimately lead to a unified three-dimensional/two-dimensional (3D/2D) calibration model of Northern Eurasia including travel times, stable coda magnitudes, and magnitude-yield relations. This model will bridge the gap between Europe, central Asia, the European Arctic, and eastern Siberia and provide additional calibration information for further work in these areas.

15. SUBJECT TERMS
Seismic attenuation, Seismic propagation, Seismic yield

16. SECURITY CLASSIFICATION OF:			17. LIMITATION OF ABSTRACT	18. NUMBER OF PAGES	19a. NAME OF RESPONSIBLE PERSON
a. REPORT	b. ABSTRACT	c. THIS PAGE	SAR	11	Robert J. Raistrick
UNCLAS	UNCLAS	UNCLAS			19b. TELEPHONE NUMBER (include area code) 781-377-3726

MAGNITUDE-YIELD AND TRAVEL-TIME CALIBRATION OF NORTHERN EURASIA USING DEEP SEISMIC SOUNDING DATA SETS

Igor B. Morozov[1], Elena A. Morozova[2], Chaoying Zhang[1], Glenn Chubak[1], W. Scott Phillips[3], and Igor A. Lipovetsky[4]

University of Saskatchewan[1], University of Wyoming[2], Los Alamos National Laboratory[3], and Center GEON/Vniigeophysika[4]

ABSTRACT

Travel-time and magnitude-yield calibration of Northern Eurasia, which is largely aseismic, can be improved by using the large chemical and peaceful nuclear explosion (PNEs) seismic data sets that resulted from the Soviet Deep Seismic Sounding (DSS) program. Eleven major data sets of this program have recently been digitized and become available to nuclear test monitoring research. In this study, we extend this database by including the source ground truth parameters (charge types, sizes, and other relevant information where available) of the chemical explosions and digitizing several earthquake data sets acquired along the DSS profiles. For seamless data exchange with the test monitoring community, we incorporate the waveforms and ancillary data into the National Nuclear Security Agency (NNSA) database schema.

To date, we have assembled a database of frequency-dependent coda parameters from the PNEs and performed their preliminary interpretation. By utilizing a newly developed, parallelized version of the one-dimensional (1D) *reflectivity* program, we also extended synthetic modeling to the full DSS frequency band (0.5-20 Hz) in velocity models of realistic crustal complexity. This modeling suggests that compared to the mantle, the crust plays the most significant role in relating the observed coda decay parameter (Q) to the intrinsic (elastic and inelastic) dependence, and also that leaking of the seismic energy into the mantle could account for the strong frequency dependence of the observed coda Q. Based on the resulting empirical relationships, we improve our previous measurements of the bulk crustal $Q(f)$ along profile QUARTZ.

In the ongoing work, we will further utilize the DSS data sets for 1) coda magnitude analysis for chemical and nuclear explosions; 2) derivation of empirical magnitude (apparent coda source spectra) yield relationships for small explosion events; and 3) examination of the variability of the derived coda calibration parameters (particularly crustal attenuation), along and across the profiles, correlating this variability with geology and tectonics of the area. Additionally, the goals of this project include derivation of a P-wave travel-time calibration model for Northern Eurasia with an unusually well-constrained and detailed crustal and uppermost mantle structure based on the chemical explosion data. These efforts should ultimately lead to a unified three-dimensional/two-dimensional (3D/2D) calibration model of Northern Eurasia including travel times, stable coda magnitudes, and magnitude-yield relations. This model will bridge the gap between Europe, central Asia, the European Arctic, and eastern Siberia and provide additional calibration information for further work in these areas.

OBJECTIVES

The general objective of this study is to derive stable and transportable regional magnitudes of smaller events and other seismic calibration information by using nuclear and chemical-explosion data sets acquired by the Russian Deep Seismic Sounding (DSS) program (Figure 1). By contrast to the paucity of natural seismicity in Northern Eurasia, DSS data sets provide unusually dense and uniform coverage of this vast area with hundreds of chemical explosions and dozens of Peaceful Nuclear Explosions (PNEs). In this report, we focus on development of approaches for coda magnitude calibration, which have been shown to yield stable magnitude/yield relationships. The specific objectives of this study are the following:

- To extend the database of DSS recordings by including the source ground truth parameters and adding several earthquake data sets acquired along the DSS profiles.

- To develop improved tools for DSS data exchange between the participants of this project and also with other users of DSS data sets.

- To develop an improved $Q(f)$ parameterization suitable for coda magnitude calibration using numerical modeling, demonstrate its physically attractive properties, and substantiate it by numerical modeling and observations.
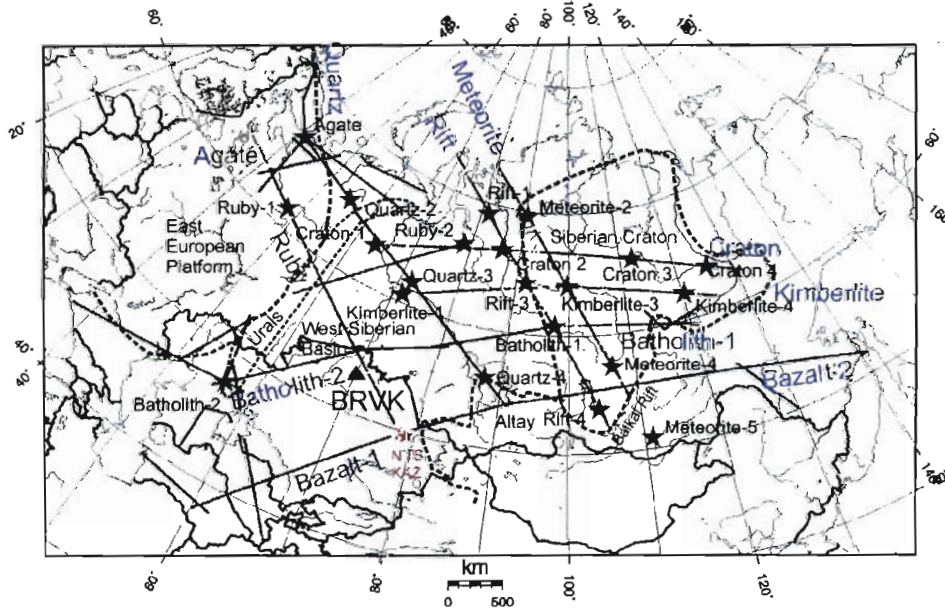
Figure 1. Location map of DSS PNE projects of this project. Projects are labeled in blue, and labeled purple stars show the PNEs. The data set also includes two Semipalatinsk nuclear test site explosions (red). Parameters of the PNEs were reported by Sultanov et al (1999). Major tectonic units are indicated in green. Small brown circles (appearing as lines at station spacing of 10-15 km) are PNE recording stations, and blue circles are chemical-explosion recording stations. Each profile also contains from 30 to 150 chemical explosions. Borovoye IMS station is also indicated (BRVK).

RESEARCH ACCOMPLISHED

Data

Because DSS data sets bridge the gap between controlled-source and earthquake seismology, data formats accepted in these areas are only marginally suitable for maintaining DSS data. The data format that we used for exporting DSS PNE over the years (an extension of PASSCAL SEGY) has caused occasional difficulties in data transfer and in a few cases required custom reformatting. The volumes of chemical-shot data sets could present significantly greater challenge in such reformatting (30-150 shots per profile as opposed to 2-4 PNEs). For seamless data exchange between the participants of this project (University of Saskatchewan and Los Alamos National Laboratory) with the test monitoring community, we incorporated the waveforms and ancillary data into the NNSA database schema. The procedure is currently undergoing extensive testing using the chemical-explosion data sets.

Center GEON (Moscow, Russia) has started digitalization of earthquake records from profiles AGATE-1 (465 seismograms), BATHOLITH-2 (135 seismograms), BAZALT-2 (680 seismograms), and QUARTZ (710 seismograms) (Figure 1). This work is currently in progress.

Coda Analysis and Modeling

To date, we have assembled a database of frequency-dependent coda parameters from the PNEs and performed their preliminary interpretation. By utilizing a newly developed, parallelized version of the 1D *reflectivity* program, we also extended synthetic modeling to the full DSS frequency band (0.5-20 Hz) and in velocity models of realistic crustal complexity.

In most cases, the *Lg* coda Q observed from earthquake and PNE records shows significant frequency dependence. This dependence could complicate coda magnitude calibration, and understanding of the processes contributing to frequency-dependent coda attenuation is critical for the development of a correct and robust calibration model. In practical terms, it is essential to develop a parameterization of the coda $Q(f)$ dependence that would reflect the fundamental physical processes and crustal properties involved. With such parameterization, the resulting calibration model would stand a better chance for being portable, and its parameters could potentially be stable across broader areas and geological environments.

The attenuation of seismic waves is usually described by the "quality" parameter Q (e.g., Knopoff, 1964). However, depending on the type of observations (e.g., body-wave, *Lg*, or coda Q) and the method used to measure Q, different energy loss mechanisms may be important, leading to different $Q(f)$ functional forms. Customarily, the frequency-dependent quality factor, $Q(f)$, is described by a two-parameter power law:

$$Q(f) = Q_0 \left(\frac{f}{f_0} \right)^{\eta} , \tag{1}$$

where f_0 is some reference frequency often taken to be 1 Hz. Both Q_0 and exponent η are considered constant (typically, $\eta > 0$) within the frequency band of interest. The power-law dependence appears to be generally dictated by convenience and represents a suitable parameterization in most cases. From several $Lg\ Q$ and Lg coda Q studies, the frequency-dependence parameter η typically ranges from ~0.1 to near 1.0 (e.g., Nuttli, 1973; Mitchell, 1975; Frankel, 1991; Benz et al., 1997; Mitchell et al., 1997, 1998; McNamara, 2001; Erickson et al., 2004). Visco-elastic rheological models were also proposed to explain observations of frequency-dependent Q in Earth materials (Liu et al., 1976). Correlation to tectonics appears to suggest that active tectonic regions are generally characterized by low Q_0 and high η, while stable cratons – by higher Q_0 and lower η (Erickson et al., 2004).

However, note that frequency-dependent Q is typically measured from the amplitude decay rates in the time domain. This method relies on the ability to accurately compensate the geometrical spreading effects, and errors in the geometrical spreading would manifest themselves as a frequency-dependent Q. Dainty (1981) suggested that for S-waves at 1-30 Hz, the observed frequency dependence could be best described using the following expression (Warren, 1972):

$$\frac{1}{Q(f)} = \frac{1}{Q} + \frac{g_0 v}{2\pi f} , \tag{2}$$

where Q is the quality factor for intrinsic (anelastic) attenuation, v is the S-wave velocity, and g_0 is the turbidity describing the elastic attenuation. If larger scatterers dominate the scattering, g_0 could be considered constant (Dainty, 1981), leading to an alternative form (2) for $Q(f)$. The second term in this expression is essentially an additional geometrical spreading (geometrical scattering) effect, which may dominate the observations (Dainty, 1981),

Although both two-parameter forms (1) and (2) can be used for describing experimental data (owing to significant uncertainties in the latter), their implications for development of suitable calibration models could be significant. In the following, we present some observations from Soviet PNEs and coda modeling results. Both of these results favor the $Q(f)$ model (2).

Observations of frequency-dependent coda Q

The initial interpretation of the frequency-dependent coda in PNE QUARTZ-4 (Morozov and Smithson, 2000) used form (1) for $Q(f)$. The measurements of Lg coda Q were performed for a location near the Mezenskaya Depression (near the position of PNE QUARTZ-2 in Figure 1), and resulted in $Q_0=350$ (at $f_0=1$ Hz) and $\eta=0.13$ in relation (1). (Figure 2; Morozov and Smithson, 2000). The somewhat low Q_0 value was explained as caused by thick sediments within the depression, and low η appeared in agreement with the stable East European Platform.
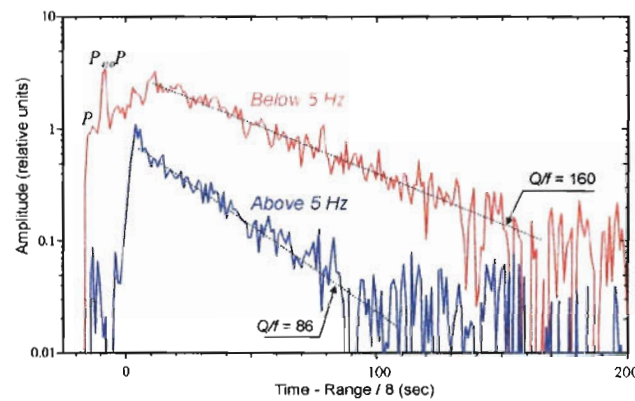
Figure 2. Amplitude-time decay for Lg coda from PNE QUARTZ-4, measured near the position of PNE QUARTZ-2 (Figure 1Error! Reference source not found.). Note the increasing amplitude decay rate with frequency; this increase is indicative of seismic attenuation. Q/f values measured from the slopes are given in the labels.

Similar measurements using the records from profiles KIMBERLITE and METEORITE in Siberia lead to strikingly different results. The logarithms of Lg coda amplitudes measured from PNE Kimberlite-3 at a station within the Siberian craton show approximately frequency-independent decays with time (Figure 3). To account for such frequency-independent decay rate in relation (1), Q should be proportional to the frequency ($\eta\approx1$). From eq. (1) Q_0 was estimated as ~200 for Lg coda and 400 for the S-wave coda, with both values appearing surprisingly low for this cratonic area and also in disagreement with observations of Pg propagating to ~1700 km in this area (Morozov et al., 2005).
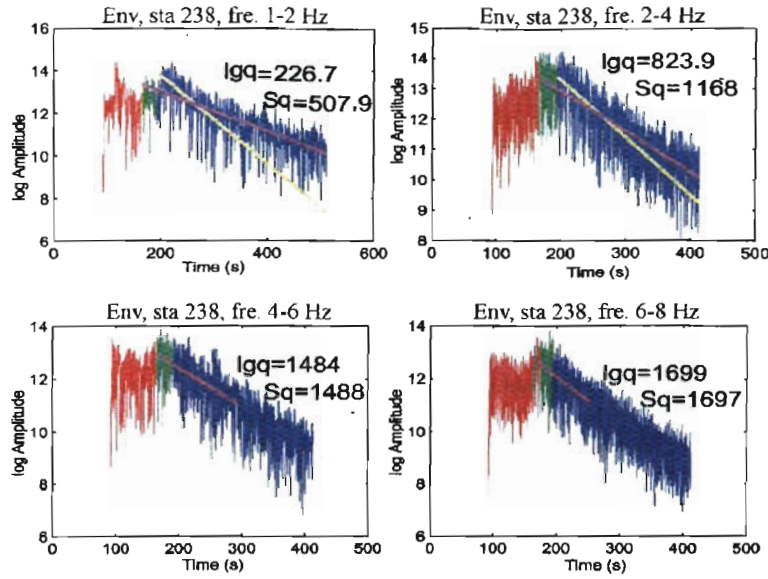
Figure 3. Amplitude envelope of vertical-component record from station 238 from PNE Kimberlie-3 filtered within 1-2, 2-4, 4-6, and 6-8 Hz frequency bands (labeled). Estimated coda Q for the S-wave and Lg coda windows are indicated. Note that these Q values quickly increase with frequency. Also note that at the same time, temporal slopes of log(amplitudes) appear to be independent on the frequency bands.

High $\eta \approx 1$ values in relation (1) would imply that attenuation is quickly reduced with frequency. As we argued previously (Morozov et al., 2005), for coda waves, attenuation decreasing with frequency would mean that the total volume of scatterers drops nearly linearly at smaller scale lengths. Although this could be possible, it still appears unlikely, as scaling laws suggest increasing abundance of heterogeneities (e.g., faults and topographic features) at smaller scales. In addition the $\eta \approx 1$ value itself appears suspicious, as it represents rather extreme case of frequency-dependent $Q(f)$ that in fact corresponds to frequency-independent amplitude decay, which could be also attributed to geometrical spreading.

To account for these observations, Morozov et al. (2005) argued that instead of the commonly used coda attenuation relation:

$$\frac{d \log A}{dt} \approx -\frac{\pi f}{Q(f)}, \tag{3}$$

a simple linear relation could be more appropriate, at least for describing the amplitude decay of PNE arrival coda:

$$\frac{d \log A}{dt} \approx -\gamma - \frac{\pi f}{Q_{coda}}. \tag{4}$$

Here, γ is the uncompensated geometrical spreading, and Q_{coda} is the attenuation parameter. Because only two parameters describing the $d \log A(f)/dt$ dependence are retained (as it is only practical in the actual measurements), the attenuation is frequency-independent. Note that the empirical expression (4) is equivalent to (2), with $\gamma = g_0 v / 2\pi$ in the case of scattering described by Dainty (1981).

Notably, application of the dependence (4) instead of (1) to QUARTZ-4 (Figure 2) and KIMBERLITE-3 (Figure 3) observations showed that for both data sets, geometrical factors were similar, $\gamma \approx 0.003$ s^{-1}, with crustal attenuation (which should predominantly be related to Q_S) $Q_{coda} \approx 470$ for QUARTZ and $Q_{coda} = \infty$ for KIMBERLITE (Morozov et al., 2005). In agreement with the observations of an unusually efficiently propagating Pg within the Siberian Craton, its crust should indeed possess a very low attenuation. Close geometrical factors both east and west of the Uralian belt (Figure 1) could also be expected, as crustal thickness is similar in both of these areas. If γ is confirmed

134

to be stable or correlated with known crustal properties, it could become a useful and transportable calibration parameter. Robust regional values of geometrical spreading could be utilized to correct the observed coda Q values (Morozov et al., 2005).

Numerical Model of Coda Q

Useful insights into the nature of a frequency-dependent coda Q can be gleaned from numerical modeling. Using synthetic modeling, one could try a range of (frequency-independent) crustal Q values, simulate the coda wavefields, measure the resulting coda amplitude decays within different frequency bands, measure the resulting coda log-amplitude slopes (4), from which the effective coda $Q_{coda}(f)$ (eq. (1)) can be estimated. Note that even for a frequency-independent crustal Q, the resulting Q_{coda} is likely to depend on the frequency - and this is confirmed by our numerical experiment below.

We re-implemented our earlier modeling attempt (Morozov et al., 2002), with modifications including an improved (parallelized) version of the one-dimensional (1D) reflectivity program (Fuchs and Muller, 1971) and utilizing a Beowulf cluster computer. These modifications allowed us to increase the frequency band to 20 Hz, offset ranges to 3000 km, and improve the sampling in Monte-Carlo computations (Morozov et al., 2002). In addition, fidelity of the synthetics (signal/numerical noise ratio) was improved by using longer modeling times and unaliased phase velocity spectra in *reflectivity* computations (Fuchs and Muller, 1971), also facilitated by code parallelization.

The modeling proceeded as follows. First, several 1D crustal and upper mantle velocity models were created. The models contained crustal layering and complex mantle structures leading to synthetic wavefields with strong and complex P, S, Pg, and Lg wavetrains. For each of these models, a range of crustal Q was tested while keeping the distribution of mantle Q as determined by Morozov et al. (1998). For each value of crustal Q, synthetic wavefields were precomputed and used as the source field u and Green's function G in the following single-scattering integral:

$$\tilde{u}_{coda}(r,t) = R \int dsdt' A(s)u(s,t') * G(s,t'\,|\,r,t),\qquad(4)$$

where s is the surface integration point, A is the scattering potential, R is the receiver site factor, and '$*$' denotes time convolution (Figure 4). For simplicity (and also recognizing that the strongest heterogeneity is located in the near-surface), scattering points were placed close to the surface, and therefore the integration was carried out over the 2-D surface of the model (Figure 4). In this simulation, the scattering potential was assumed uniform, $A(s)=1$, and only one receiver position at 2900 km from the source was considered. Integration (4) was performed using the Monte-Carlo method, by random sampling of the 2500-km square in 30 parallel runs of the code with 2000 scattering points in each of run (Figure 4).
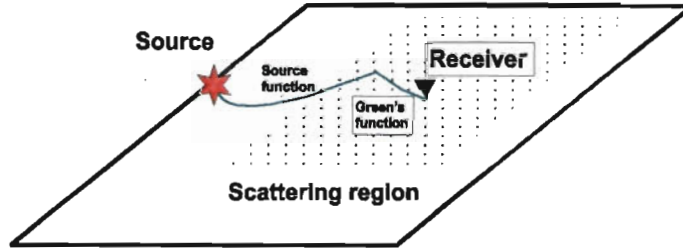

Figure 4. Surface scattering model. Seismic energy originates at the source, scatters from uniformly distributed Monte-Carlo-sampled surface points, and is detected at receiver. Source and Green's functions are precomputed using the 1-D reflectivity approach (Fuchs and Muller, 1971).

Because of the wavefield complexity, the scattered field is also very complex and consists of an interplay of various scattering modes ($P{\to}P$, $P{\to}Pg$, $S{\to}P$, etc.) (Figure 4). However, fortunately for our analysis, different source phases are incoherent between each other, and consequently the power (intensity) of the scattered wavefield (4) is the sum of the intensities of the field caused by the different source phases. Therefore, the different primary arrivals can be considered independently, in a way similar to the coda decomposition model by Morozov and Smithson (2000). Below, we only consider the coda of the source P-wave, which was obtained by muting the source $u(s,t)$ in

expression (4) leaving only the time window corresponding to the primary body P-wave arrival. The results should thus represent the dependence of the P-wave coda Q on crustal Q and frequency, even though the P-wave coda is usually overprinted with secondary events and is difficult to measure from PNE data (Morozov and Smithson, 2000).

Below, we present numerical tests using two crustal/mantle models: "Quartz-4," based on the structure derived from 2D inversion of PNE profile QUARTZ (Morozova et al., 1999) and the same model with crustal complexity (layering) increased by introduction of a lower-velocity sedimentary layer and increased intracrustal contrasts and gradient in the uppermost mantle (Figure 5). In this model, a greater portion of the energy should return to the surface earlier. Examples of the Green's function sections for the "complex crust" model within two frequency bands are shown in Figure 6. Note the dependence of the Green's functions on the frequency.
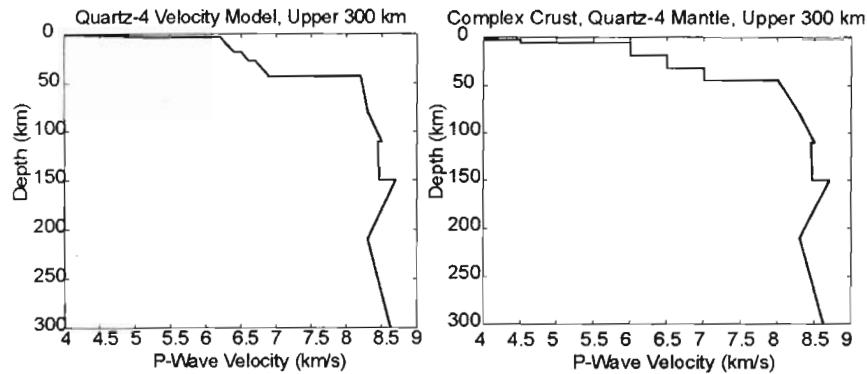

Figure 5. Upper 300 km of 1D velocity models discussed in this report. *Left*: PNE Quartz-4 model by Morozova et. al. (1999). *Right*: "complex crust" model, with modified 5-layer crust and Quartz-4 mantle with somewhat increased gradient in the uppermost mantle gradient.
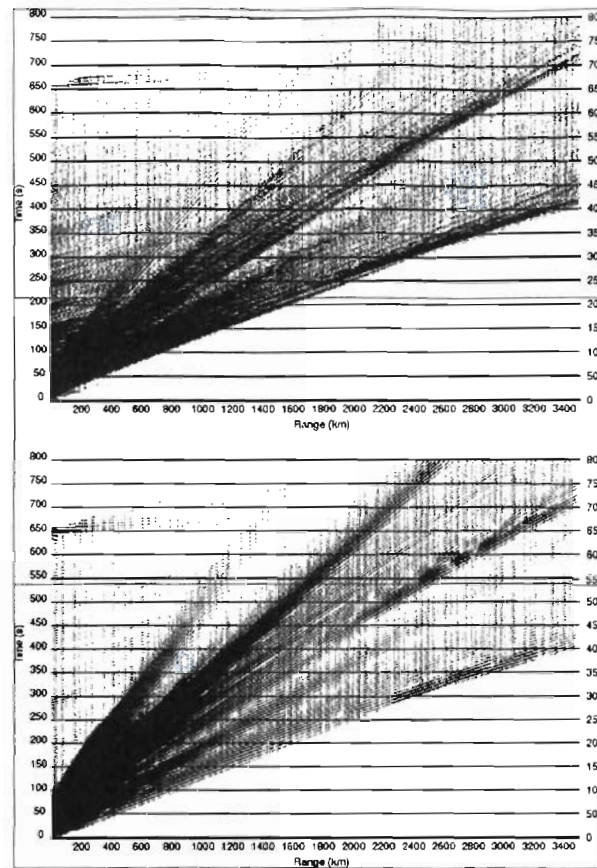
Figure 6. Synthetic Green's function computed using the "complex crust" model (Figure 4). *Top*: unfiltered vertical-component records; *Bottom*: the same record filtered within 0.1-0.2 Hz frequency band.

The dependence of the logarithms of the resulting coda amplitudes at the receiver (Figure 4) on recording time for crustal Q=550 in the "complex crust" is shown in Figure 7. This plot was obtained by computing logarithms of instantaneous amplitudes (envelopes) of the records obtained from each of the ~30 statistical simulations, followed by stacking the resulting logarithms. The resulting records show very good continuity and linearity, and the slopes can be measured with ~1% accuracy using the standard linear regression (Figure 7). We found that this approach serves as a good proxy for robust regression.
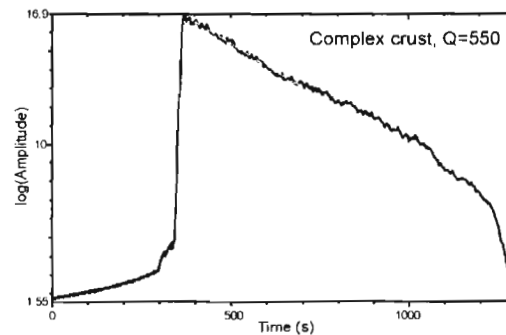
Figure 7. Modelled *P*-wave coda in the "complex crust" model. Note the linear slope allowing accurate $\log(A)/dt$ measurements (dashed red line).

By filtering the resulting coda synthetics (prior to stacking described above) within narrow pass-bands, frequency-dependent coda slopes similar to the one shown in Figure 7 were produced. By using relation (3), these slopes were transformed into coda Q values shown in Figure 8. In all cases we have studied so far, and similarly to PNE observations above, the resulting Q_{coda} values are nearly proportional to the frequency (Figure 8).
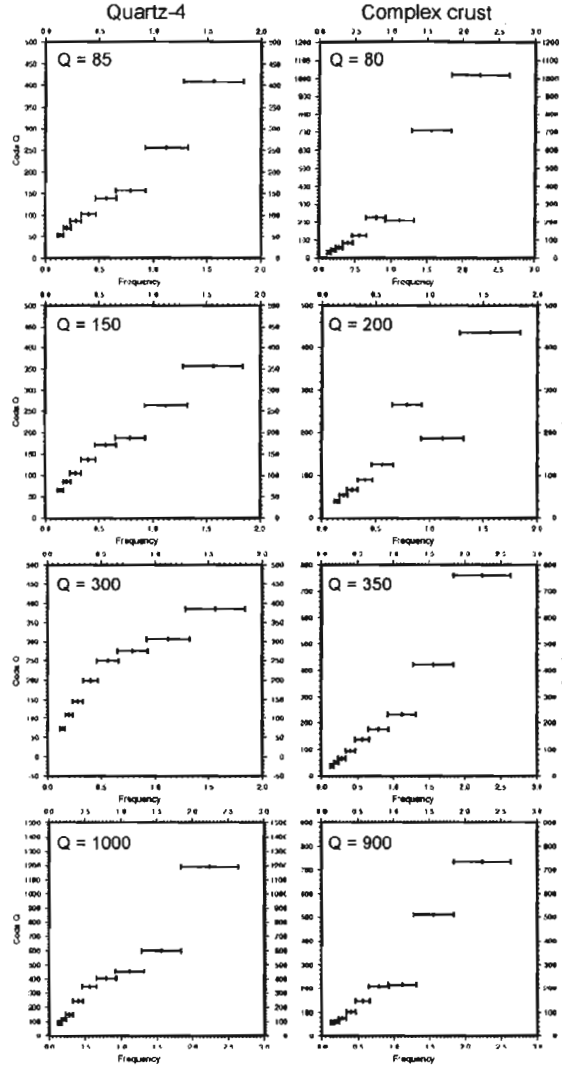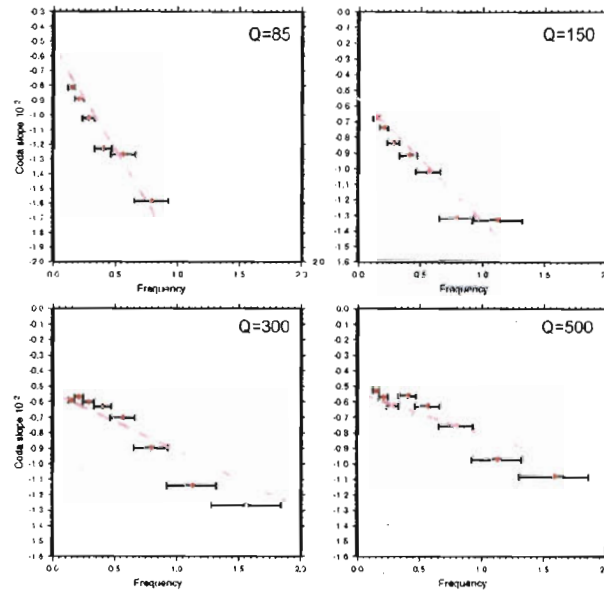

Figure 8. Coda Q as functions of frequency, inverted from the synthetic coda log-amplitude slopes using relation (3). Note the near-linear frequency dependence of $Q_{coda}(f)$. Error bars represent bandwidths of the filters applied to the synthetics.

Interpretation

Because our rheological models contain no relaxation mechanisms, attenuation in all parts of the models should be frequency-independent. The strong positive frequency dependence observed in the models (Figure 8) suggests that the high-frequency energy propagates to farther distances more efficiently than by traveling through the attenuating crust. This means that the coda amplitude decay (Figure 7) is controlled more by geometrical factors (refraction into the mantle, scattering on crustal discontinuities) than by anelastic attenuation. Consequently, although taken as empirical descriptions of the coda variation with frequency, $Q_{coda}(f)$ dependencies (Figure 8) provide a description of the observations, and Q_{coda} values themselves could still be difficult to relate to any meaningful crustal rheology.

Therefore, their value for seismic calibration and regionalization could also be difficult to ascertain without a detailed knowledge of the crustal structure and extensive modeling.

By contrast, direct comparison of the original coda log-amplitude slope measurements (Figure 7) shows that the synthetics are consistent with equations (2) and (4) (Figure 9). For Quartz-4 model, the time-frequency behavior of coda amplitudes can be explained by the geometrical spreading (elastic attenuation, cf. Dainty 1981) factor $\gamma \approx 0.55$ and $Q_{coda} \approx 2.5\ Q$ [eq. (4)]). Note that as expected, the coda Q is higher than the crustal S-wave and P-wave Q's used to parameterize the model, apparently because part of the energy propagates through the mantle, which has lower attenuation. Factor 2.5 relating the crustal Q to Q_{coda} should apparently depend on the structure; detailed analysis of this dependence will be addressed in further research.

Figure 9. Logarithmic coda amplitude slopes as functions of frequency in Quartz-4 model. Dashed pink lines correspond to dependence (4) with $\gamma = 0.55$ and $Q_{coda} = 2.5\ Q$.

CONCLUSIONS AND RECOMMENDATIONS

Analysis of the frequency-dependent Lg coda Q from DSS PNE profiles indicates significant differences in attenuation properties between the East European Platform and West Siberian Basin and Siberian Craton. To explain these variations, we propose to abandon the customary $Q(f) = Q_0 f^{\eta}$ model for frequency-dependent coda attenuation and use geometrical spreading and frequency-independent attenuation. In this model, the geometrical spreading is consistent between the two studied areas, and the attenuation appears to be very low within the Siberian Craton, in agreement with other observations.

The proposed coda model was tested by numerical modeling of P-wave coda in PNE wavefields. Coda synthetics computed using a velocity, attenuation, and density structure close to that of the East European Platform and SW part of the West Siberian Basin show good correspondence with the model. Modeling results show that the geometric spreading factor for this area equals approximately 0.55, and the effective coda Q is approximately 2.5 times the crustal S-wave Q. These results suggest that 1) geometrical spreading (elastic attenuation) dominates PNE coda amplitudes decays, 2) the observed coda Q_{coda} derived by using the modified model could be useful to constrain the intrinsic crustal Q, and 3) modeling should be used to calibrate the $Q_{coda}(Q)$ dependence that should be also related to the crustal structure.

REFERENCES

Benz, H., A. Frankel, and D. Boore (1997). Regional Lg attenuation in the continental United States, *Bull. Seis. Soc. Am.* 87: 600–619.

Erickson, D., D. E. McNamara, and H. Benz (2005). Frequency-dependent Lg Q within the continental United States, *Bull. Seism. Soc. Am.* 94: 1630–1643.

Frankel, A. (1991). Mechanism of seismic attenuation in the crust: scattering and inelasticity in New York state, South Africa, and southern California, *J. Geophys. Res.*, 96, 17441-17457.

Fuchs, K., and G. Müller, (1971). Computation of synthetic seismograms with the reflectivity method and comparison with observations, *J. R. Astronom. Soc.*, *23*, 417–433

Knopoff, L. (1964). *Rev. Geophys.* 2: 625-660.

Liu, H. P., Anderson, D. L., Kanamori, H. (1976). Velocity dispersion due to anelasticity: implications for seismology and mantle composition, *Geophysical Journal of the Royal Astronomical Society* 47: 41–58.

McNamara, D. E. (2000). Frequency-dependent *Lg* attenuation in south-central Alaska, *Geophys. Res. Lett.* 27: 3949–3952.

Mitchell, B. (1975). Regional Rayleigh wave attenuation in North America, *J. Geophys. Res.*, 80: 4904–4916.

Mitchell, B. J., Cong, L. (1998). *Lg* coda Q and its relation to the structure and evolution of continents: a global Perspective, *Pure Appl. Geophys.* 153: 655–663.

Mitchell, B. J., Pan, Y., Xie, J., Cong, L. (1997). *Lg* coda Q variation across Eurasia and its relation to crustal evolution, *J. Geophys. Res.* 102: 22767–22779.

Morozov, I. B., and S. B. Smithson (2000). Coda of long-range arrivals from nuclear explosions, *Bull. Seism. Soc. Am.* 90: 929–939.

Morozov, I. B., E. A. Morozova, S. B. Smithson, and L. N. Solodilov, (1998). 2-D image of seismic attenuation beneath the Deep Seismic Sounding profile "Quartz", Russia, *Pure and Applied Geoph.* 153: 311–348.

Morozov, I. B., Smithson, S. B., Li, H., and Duenow, J. N. (2002). Amplitude analysis and modeling of peaceful nuclear explosion recordings, in *Proceedings of 24th Seismic Research Review—Nuclear Explosion Monitoring: Innovation and Integration,* LA-UR-02-5048, Vol. 1, pp. 117–124.

Morozov, I., Li, H., Zheng, H., and Smithson, S. B. (2005). Observations and modeling of frequency-dependent lg coda from Peaceful Nuclear Explosions, in *Proceedings of 27th Seismic Research Review: Ground-Based Nuclear Explosion Monitoring Technologies,* LA-UR-05-6407, Vol. 1, 104–112.

Morozova, E. A., I. B. Morozov, S. B. Smithson, and L. N Solodilov (1999). Heterogeneity of the uppermost mantle beneath the ultra-long range profile "Quartz," Russian Eurasia, *J. Geophys. Res.* 104: (B9), 20: 329–20, 348.

Nuttli, O. (1973). Seismic wave attenuation and magnitude relations for eastern North America, *J. Geophys. Res.*, 78: 876–885.

Schueller, W., I. B. Morozov, and S. B. Smithson (1997). Crustal and uppermost mantle velocity structure of northern Eurasia along the profile Quartz, *Bull. Seism. Soc. Am.* 87: 414–426.

Sultanov, D. D., J. R. Murphy, and Kh. D. Rubinstein (1999). A seismic source summary for Soviet Peaceful Nuclear Explosions, *Bull. Seism. Soc. Am.* 89: 640–647.

Warren, N. (1972). Q and structure, *Earth, Moon, and Planets*, 4: (3-4), 430–441, Springer Netherlands.